Enhanced Spin Conductance of a Thin-Film Insulating Antiferromagnet

Scott A. Bender,[1] Hans Skarsvåg,[2] Arne Brataas,[2] and Rembert A. Duine[1,3]
[1]Utrecht University, Princetonplein 5, 3584 CC Utrecht, Netherlands
[2]Department of Physics, Norwegian University of Science and Technology, NO-7491 Trondheim, Norway
[3]Department of Applied Physics, Eindhoven University of Technology, P.O. Box 513, 5600 MB Eindhoven, The Netherlands
(Received 6 February 2017; published 4 August 2017)

We investigate spin transport by thermally excited spin waves in an antiferromagnetic insulator. Starting from a stochastic Landau-Lifshitz-Gilbert phenomenology, we obtain the out-of-equilibrium spin-wave properties. In linear response to spin biasing and a temperature gradient, we compute the spin transport through a normal-metal–antiferromagnet–normal-metal heterostructure. We show that the spin conductance diverges as one approaches the spin-flop transition; this enhancement of the conductance should be readily observable by sweeping the magnetic field across the spin-flop transition. The results from such experiments may, on the one hand, enhance our understanding of spin transport near a phase transition, and on the other be useful for applications that require a large degree of tunability of spin currents. In contrast, the spin Seebeck coefficient does not diverge at the spin-flop transition. Furthermore, the spin Seebeck coefficient is finite even at zero magnetic field, provided that the normal metal contacts break the symmetry between the antiferromagnetic sublattices.

DOI: 10.1103/PhysRevLett.119.056804

Introduction.—Antiferromagnets have recently garnered increasing interest in the spintronics community, for both their novel intrinsic properties and their technological potential. Their appealing features are their lack of stray magnetic fields, fast dynamics relative to ferromagnets, and robustness against external fields [1]. The last property is a double-edged sword, as the lack of response to an external field makes control of antiferromagnets challenging. Recent theoretical and experimental work has instead sought to generate and detect antiferromagnetic dynamics optically [2] and electrically [3].

Spin transport through insulators is of particular interest because there is no dissipation associated with the motion of electrons. However, there is currently a lack of understanding of how spins can flow between metals via antiferromagnetic insulators. Exploring these phenomena is essential for exploiting antiferromagnetic insulators in a more active role in spintronics. In ferromagnets, equilibrium thermal fluctuations generate spin waves that can drive coherent magnetic dynamics [4] or transport spins [5]. For instance, a nonlocal spin conductance contains signatures of the spin transport properties. Measurements of this spin conductance have generated considerable excitement in the spintronics community [5]. It is of interest to see if thermal magnons can provide a similar long-range spin transport in antiferromagnetic insulators. We predict that the spin conductance is as substantial in antiferromagnets and therefore expect that thermal magnon transport in these systems will generate a sizable interest as well. Below we discuss in detail two scenarios to open the door for long-range spin transport through antiferromagnetic insulators, without the need for adjacent ferromagnets, or, in principle, magnetic fields.

In antiferromagnets, at zero magnetic fields, spin-wave excitations are doubly degenerate. The two branches carry opposite spin polarity. Thus, to realize spin transport by thermally generated spin waves, the symmetry between the antiferromagnetic sublattices must be lifted. One means of achieving this is to employ a ferromagnetic layer, controlled by a magnetic field [6]. Alternatively, the magnetic field itself suffices to break the sublattice symmetry, eliminating the need for a ferromagnetic component. Reference [7] measured the spin Seebeck effect [8,9], in which angular momentum is driven by a temperature gradient in bipartite electrically insulating antiferromagnets at finite magnetic fields.

The first scenario is the injection of thermal magnons by a spin accumulation in an adjacent metal. While spin-accumulation-induced thermal magnon injection in ferromagnet–normal-metal heterostructures has been the subject of recent theoretical research [10,11], predictions for the antiferromagnetic analogue are currently lacking and are restricted to coherent magnetic dynamics of the antiferromagnetic order and the resulting spin superfluidity that requires external fields [12,13]. Here, we show that the spin conductivity of thermal magnons is strongly enhanced upon approaching the spin-flop transition. This leads to a large amount of tunability of the magnon transport by an external field, which may be desirable for applications.

A second possibility for engineering magnon spin transport in antiferromagnets is to break the interface sublattice symmetry. Magnetically uncompensated antiferromagnet-metal interfaces have been studied theoretically [14]. Nevertheless, the possibility of realizing a spin Seebeck effect by breaking the sublattice symmetry at the interface has not been proposed until now.

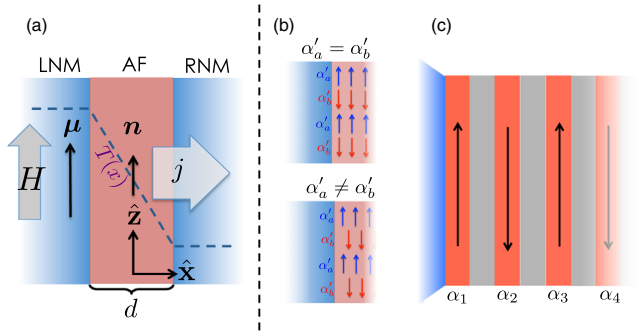

FIG. 1. (a) LNM-AF-RNM setup. A spin accumulation $\boldsymbol{\mu} = \mu\mathbf{z}$ at the left interface inside the left normal metal and temperature gradient $\partial_x T$ across the heterostructure are applied; as a result a spin current j flows across the right interface. (b) Metal-antiferromagnet interface, with unbroken ($\alpha'_a = \alpha'_b$, top) and broken ($\alpha'_a \neq \alpha'_b$, bottom) sublattice symmetries. (c) Symmetry breaking in a synthetic antiferromagnet, composed of alternating metallic spacers and ferromagnetic layers with respective damping parameters α_1, α_2…. If, for example, the contact (blue) material differs from that of the interlayer spacer (gray), then $\alpha_1 \neq \alpha_2$, analogously to (b).

Stochastic dynamics.—We consider a bipartite antiferromagnet (AF). The system is translationally invariant in the yz plane. There is an interface along the plane $x = -d/2$ on the left with a normal metal (LNM) and an interface along the plane $x = d/2$ with an identical normal metal (RNM) on the right [see Fig. 1(a)]. Let us suppose that a spin accumulation $\boldsymbol{\mu} = \mu\hat{\mathbf{z}}$ is fixed by, e.g., spin Hall physics in the left lead, or that a linear phonon temperature profile is established across the structure [15].

We begin by parameterizing the AF spin degrees of freedom in the long wavelength limit by the Néel order unit vector $\mathbf{n}$ and dimensionless magnetization $\mathbf{m}$. At zero temperature, the AF relaxes towards a ground state determined by the free energy U [16],

$$U = s\int_{\mathcal{V}} d^3r\left(\frac{\mathbf{m}^2}{2\chi} + \frac{A}{2}\sum_{i=1}^{3}(\partial_i\mathbf{n})^2 - \frac{1}{2}Kn_z^2 - \mathbf{H}\cdot\mathbf{m}\right). \quad (1)$$

Here, $s = s_a + s_b$ is the sum of the saturation spin densities of the a and b sublattices (in units of $\hbar$), $\mathcal{V}$ is the volume of the AF, χ is the susceptibility, A is the Néel order exchange stiffness, and $K(>0)$ is the uniaxial, easy-axis anisotropy. The external magnetic field $\mathbf{H}$ is taken to be applied along the z direction in order to preserve rotational symmetry around the z axis in spin space. The bulk symmetry of the bipartite lattice under the interchange of the sublattices, which sends $\mathbf{m} \to \mathbf{m}$ and $\mathbf{n} \to -\mathbf{n}$, is manifest in the form of U.

At sufficiently small magnetic fields, $|H| < H_c = \sqrt{K/\chi}$, the ground states are degenerate, given by $\mathbf{n} = \pm\mathbf{z}$ and $\mathbf{m} = 0$, and the AF is in the antiferromagnetic phase. In the antiferromagnetic phase, the ground state magnetic texture is insensitive to the spin accumulation $\boldsymbol{\mu}$ in the linear response, and the AF does not support a spin current at zero temperature. At fields $|H| > H_c$, the ground state is "spin-flopped," with $\mathbf{m} \propto \mathbf{z}$ and $\mathbf{n}$ in the xy plane. Spin biasing of the spin-flopped state generates a spin super current [12,13] at zero temperature. In order to focus on transport by thermally activated spin waves, we restrict the following discussion to the antiferromagnetic phase. Furthermore, in this phase, the spin waves are circular and therefore simpler to analyze.

At finite temperatures, fluctuations drive the AF texture away from the zero-temperature configuration, necessitating equations of motion that incorporate bulk and boundary fluctuations and dissipation. The small amplitude excitations of the Néel order above the ground state $\mathbf{n} = -\mathbf{z}$ are $\delta\mathbf{n}$, described by the linearized equation of motion in the bulk ($-d/2 < x < d/2$),

$$(\partial_x^2 + \mathfrak{q}^2)n = -\mathfrak{f}_B/A. \quad (2)$$

(see Supplemental Material [17]). Here, $n = n(x, \mathbf{q}, \omega)$ is the Fourier transform (in the coordinates $\boldsymbol{\rho} = y\hat{\mathbf{y}} + z\hat{\mathbf{z}}$ and t) of $n(x, \boldsymbol{\rho}, t) \equiv n_x(x, \boldsymbol{\rho}, t) + in_y(x, \boldsymbol{\rho}, t)$, while $\mathfrak{q}^2 \equiv -\mathbf{q}^2 - K/A + \eta_\omega^2/A\chi + i\alpha\hbar\omega/A$ with $\eta_\omega \equiv \chi(\hbar\omega + H)$. The stochastic force $\mathfrak{f}_B$, modeling fluctuations of the AF lattice that drive n, is connected to the bulk Gilbert damping α by the fluctuation dissipation theorem (here in the large exchange regime, $\chi^{-1} \gg \hbar\omega + H$),

$$\langle \mathfrak{f}_B^*(x, \mathbf{q}, \omega)\mathfrak{f}_B(x', \mathbf{q}, \omega')\rangle = \times\delta(x - x')\delta(\mathbf{q} - \mathbf{q}')\delta(\omega - \omega')\frac{2\alpha(2\pi)^3\hbar\omega}{\tanh[\hbar\omega/2T]}, \quad (3)$$

where $T = T(x)$ is the local temperature in units of energy.

Complementing Eq. (2) are boundary conditions on n,

$$\begin{aligned} A\partial_x n + i\alpha'_\omega d(\hbar\omega - \mu)n &= -\mathfrak{f}_L \quad (x = -d/2) \\ -A\partial_x n + i\alpha'_\omega d\hbar\omega n &= -\mathfrak{f}_R \quad (x = d/2), \end{aligned} \quad (4)$$

where $\mathfrak{f}_L$ and $\mathfrak{f}_R$ correspond to fluctuations by lead electrons at the interfaces. The quantity $\alpha'_\omega \equiv \alpha' - \eta_\omega\tilde{\alpha}'$, describing dissipation of magnetic dynamics at the interfaces (which we have taken to be identical for simplicity), has contributions from both sublattice-symmetry-respecting (α') and -breaking ($\tilde{\alpha}'$) microscopics there. For example, in a simple model in which fluctuation and dissipation torques for the two sublattices are treated independently (see Supplemental Material [17]), one finds $\alpha' = (\alpha'_a + \alpha'_b)/2$ and $\tilde{\alpha}' = (\alpha'_a - \alpha'_b)/2$; here $\alpha'_\zeta = g_\zeta^{\uparrow\downarrow}/4\pi sd$ (with $g_\zeta^{\uparrow\downarrow}$ as the spin-mixing conductance) is the effective damping due to spin pumping for sublattice $\zeta = a, b$ [12,14] [see Fig. 1(b)]. Such a model corresponds to the continuum limit of a synthetic antiferromagnet (composed of ferromagnetic macrospins separated by normal metals) in which sublattice

symmetry breaking may be more carefully controlled [see Fig. 1(c)].

The effective surface forces $\mathfrak{f}_{L(R)}$ and damping coefficient α'_ω are connected via the fluctuation-dissipation theorems for the $l = L, R$ interfaces,

$$\langle \mathfrak{f}_l^*(\mathbf{q},\omega)\mathfrak{f}_{l'}(\mathbf{q},\omega')\rangle = \times\delta_{ll'}\delta(\mathbf{q}-\mathbf{q}')\delta(\omega-\omega')\frac{2s\alpha'_\omega(2\pi)^3(\hbar\omega-\mu_l)}{\tanh[(\hbar\omega-\mu_l)/2T_l]}, \quad (5)$$

where we have retained terms up to first order in η_ω. Here T_L and T_R are lead electronic temperatures and, in our setup, $\mu_L = \mu$ and $\mu_R = 0$.

Spin transport.—We now obtain the spin current that flows across the right interface in linear response to the spin accumulation $\boldsymbol{\mu} = \mu\hat{\mathbf{z}}$ at the left interface. Rewriting the equation of motion for the magnetization $\mathbf{m}$ [Eq. (2) in the Supplemental Material [17]] as a continuity equation for the spin density $\mathbf{s} = s\hbar\mathbf{m}$, one obtains an expression for the spin current, $\mathbf{j} = -sA\mathbf{n}\times\partial_x\mathbf{n}$. Solving Eqs. (2)–(5) in the absence of a temperature gradient, retaining terms only up to linear order in μ, the z-spin current flowing through the right interface becomes

$$j \equiv \langle\hat{\mathbf{z}}\cdot\mathbf{j}\rangle = As\mathrm{Im}\langle n^*(\mathbf{r})\partial_x n(\mathbf{r})\rangle_{x=d/2} = G\mu, \quad (6)$$

where we have introduced the spin conductance G.

In the low-damping or thin-film limit, $d \ll \lambda$, where $\lambda^2 \equiv A/\alpha T$ is the imaginary correction to $\mathbf{q}^2$ (i.e., $\mathbf{q}^2 = q_r^2 + i\lambda^{-2}$ with q_r real) due to Gilbert damping, the spin current is carried by well-defined spin-wave modes [corresponding to solutions to Eq. (2) in the absence of noise] with frequencies $\omega_{l\mathbf{q}}^{(\pm)} = -H/\hbar \pm \hbar^{-1}\sqrt{[A\mathbf{q}^2 + A(l\pi/d)^2 + K]/\chi}$. Here $\mathbf{q}$ is the transverse wave vector, l is an integer denoting spin-wave confinement in the x direction, and the labels $\pm$ corresponds to the two spin-wave branches for which $\mathbf{n}$ rotates in opposite directions, as $\omega_{l\mathbf{q}}^{(+)}$ has the opposite sign of $\omega_{l\mathbf{q}}^{(-)}$ (though a different magnitude when $H \neq 0$). In the low-damping or thin-film limit, the spin conductance G is therefore a sum over contributions from each of these modes and can further be broken into "symmetric" and "antisymmetric" (under interchange of the sublattices) pieces,

$$G = \sum_{l=0,1,2,\ldots}\int\frac{d^2q}{(2\pi)^2}(G_{l\mathbf{q}}^{(\mathrm{S})} + G_{l\mathbf{q}}^{(\mathrm{A})}). \quad (7)$$

Defining

$$F_\pm^{(i,j)}(\xi/T) \equiv \frac{(T/\xi)^i(\hbar\omega^{(\pm)}/T)^{1+j}}{\sinh^2(\hbar\omega^{(\pm)}/2T)}, \quad (8)$$

with $\hbar\omega^{(\pm)} = -H \pm \xi$, the symmetric contribution, which is proportional to α', is

$$G_{l\mathbf{q}}^{(\mathrm{S})} = \frac{(\varsigma_l\alpha')^2}{2\varsigma_l\alpha' + \alpha}\left(\frac{1}{\chi T}\right)\mathcal{G}^{(\mathrm{S})}(\xi_{l\mathbf{q}}/T), \quad (9)$$

where $\xi_{l\mathbf{q}} \equiv \sqrt{A(\mathbf{q}^2 + [l\pi/d]^2)/\chi + K/\chi}$ and $\mathcal{G}^{(\mathrm{S})}(\xi/T) = F_+^{(1,0)}(\xi/T) - F_-^{(1,0)}(\xi/T)$, with $\varsigma_l = 1$ for $l = 0$ and $\varsigma_l = 2$ for $l > 0$ (reflecting the exchange boundary conditions [18,19]). The antisymmetric piece, which is proportional to $\tilde{\alpha}'$, reads

$$G_{l\mathbf{q}}^{(\mathrm{A})} = \varsigma_l\tilde{\alpha}'\frac{2\varsigma_l\alpha'(\varsigma_l\alpha'+\alpha)}{(2\varsigma_l\alpha'+\alpha)^2}\mathcal{G}^{(\mathrm{A})}(\xi_{l\mathbf{q}}/T), \quad (10)$$

where $\mathcal{G}^{(\mathrm{A})}(\xi/T) = F_+^{(0,0)}(\xi/T) + F_-^{(0,0)}(\xi/T)$ and we have assumed that $\tilde{\alpha}' \lesssim \alpha'$. From Eqs. (9) and (10) we find an algebraic decay of the spin current with film thickness. In the extreme thin-film limit, $d \ll g^{\uparrow\downarrow}/4\pi s\alpha$, the damping at the interface dominates over bulk, and both contributions decay as $1/d$; in the opposite regime, $d \gg g^{\uparrow\downarrow}/4\pi s\alpha$, one has that both again decay in the same way, as $1/d^2$. The symmetric and antisymmetric contributions may instead be distinguished by reversing the direction of the applied field: $\mathcal{G}^{(\mathrm{A})}(\xi/T)$ changes sign under $H \to -H$ (and therefore vanishes at zero field), while $\mathcal{G}^{(\mathrm{S})}(\xi/T)$ remains the same. Note, however, that the antisymmetric contribution, Eq. (10), is suppressed by a factor of $T\chi \ll 1$ relative to the symmetric contribution, Eq. (9).

As a consequence of the divergence of the Bose-Einstein distribution at zero spin-wave gap (and as a precursor to superfluid transport [12]), the spin conductance diverges as one approaches the spin-flop transition. The boundary for the antiferromagnetic phase is defined by the vanishing of the spin-wave gap for one of the modes ($\hbar\omega_{\mathbf{00}}^{(\pm)} = 0$), which determines the critical field, $H_c = \sqrt{K/\chi}$. Then, from Eqs. (9) and (10), both the symmetric and antisymmetric contributions diverge as $1/(1-|H|/H_c)$ as $H \to H_c$ (see Fig. 2). This enhancement of the spin-wave conductance is a key feature of spin transport in antiferromagetic insulators with a spin-flop transition.

We may compare these results with spin transport driven by a temperature gradient. Supposing a linear temperature gradient $T(x) = T + (\partial_x T)x$, with a continuous profile across the structure so that $T_L = T - \partial_x T d/2$ and $T_R = T + \partial_x T d/2$, Eqs. (2)–(5) yield a spin current for $\mu = 0$,

$$j = -S\Delta T, \quad (11)$$

where $\Delta T = d\partial_x T$ is the temperature change across the AF. In the low-damping or thin-film limit, the Seebeck coefficient S similarly separates into symmetric and antisymmetric sums over discrete spin-wave modes,

$$S = \sum_{l=0,1,2,\ldots}\int\frac{d^2q}{(2\pi)^2}(S_{l\mathbf{q}}^{(\mathrm{S})} + S_{l\mathbf{q}}^{(\mathrm{A})}), \quad (12)$$

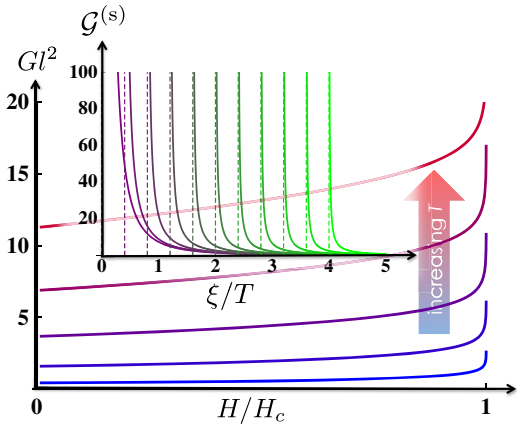

FIG. 2. Total conductance G times $l^2 \equiv A\chi$ for $\chi^{-1} = 10H_c$, $d = l$, $\alpha = \alpha' = \tilde{\alpha}' = 0.1$, for varying temperatures T/H_c from 1 to 5 in steps of 1. Inset: Symmetric magnon conductance $\mathcal{G}^{(S)}$ [defined below Eq. (9)] for a single magnon mode with energy $\hbar\omega^{(+)} = -H + \xi$ as a function of ξ for fixed temperature T. As $\xi \to H$, corresponding to the closing of the magnon gap ($H \to H_c$) and thus approaching the spin-flop transition, the conductance diverges. Shown are different fields (corresponding to the vertical dashed lines) for 0 to H_c in steps of $T/10$, with the corresponding curves for $\mathcal{G}^{(S)}$ shown in shades of purple to green. $\mathcal{G}^{(A)}$ is qualitatively similar and therefore not shown.

where

$$S^{(S)}_{l\mathbf{q}} = (\varsigma_l \alpha'/8)(1/\chi T)\mathcal{S}^{(S)}(\xi_{l\mathbf{q}}/T) \tag{13}$$

is the symmetric contribution, with $\mathcal{S}^{(S)}(\xi/T) \equiv F^{(1,1)}_{+}(\xi/T) - F^{(1,1)}_{-}(\xi/T)$, and

$$S^{(A)}_{l\mathbf{q}} = \varsigma_l(\tilde{\alpha}'/4)\mathcal{S}^{(a)}(\xi_{l\mathbf{q}}/T) \tag{14}$$

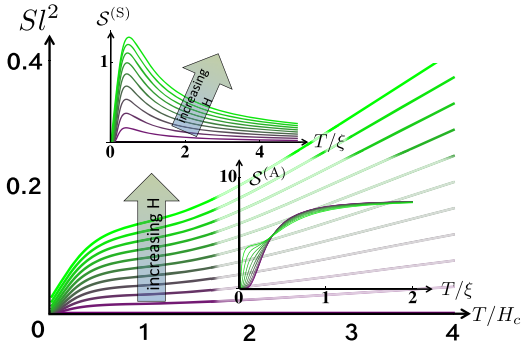

FIG. 3. Total spin Seebeck coefficient S for the symmetric case ($\tilde{\alpha}' = 0$), Eq. (12) for $\alpha' = 0.1$, $d = l = \sqrt{A\chi}$, and $\chi^{-1} = 10H_c$. $\mathcal{S}^{(S)}$ (upper inset) and $\mathcal{S}^{(A)}$ (lower inset) as functions of temperature for fixed ξ. While the symmetric contribution vanishes at high temperatures, the antisymmetric contribution saturates at $\mathcal{S}^{(A)} = 8$. The solid purple or green curves correspond to H ranging from 0 to H_c in increments of $H_c/10$. At high temperatures, S grows larger with temperature, in contrast with [7,9]; see second section of Supplemental Material [17].

the antisymmetric contribution, with $\mathcal{S}^{(A)}(\xi/T) \equiv F^{(0,1)}_{+}(\xi/T) + F^{(0,1)}_{-}(\xi/T)$ (see Fig. 3). In contrast to the spin conductance, there is no divergence in the spin Seebeck coefficient as $H \to H_c$. Furthermore, the antisymmetric contribution is even under $H \to -H$ (and is generally nonzero at zero field), while the symmetric contribution is odd (vanishing at zero field, as is required by sublattice symmetry); in contrast to spin biasing, a temperature gradient requires either a field or sublattice symmetry breaking at the interfaces in order to generate a spin current, else the two branches $\pm$ carry equal and opposite spin currents. Both symmetric and antisymmetric contributions to S decay as $1/d$; writing $j = S\Delta T = \varsigma\partial_x T$, one finds that $\varsigma \equiv Sd$ is constant, reflecting that the Seebeck effect here is driven by bulk fluctuations.

The transport coefficients G and S may be inferred from a number of different experiments. Suppose, for example, the leads are heavy metal with large spin-orbit interactions. The spin conductance G may then be measured electrically as follows. Via the spin Hall effect, a spin accumulation is created in the LNM from an applied electric current I_L flowing in the y direction. In turn, the spin accumulation excites spin waves in the AF, as described above. Via the inverse spin Hall effect, this spin current is then converted to a measurable electrical current flowing in the y direction inside the RNM. Under closed-circuit conditions, this current manifests as a voltage buildup V_R. For a platinum-MnF_2-platinum structure, we find a nonlocal resistance $R = V_R/I_L \sim m\Omega$ from our theory, which is of the same order of magnitude as that measured in [10] for a ferromagnet. Similarly, for the same setup, the Seebeck coefficient S can be obtained by applying a temperature difference across the structure. We estimate that a temperature difference of $\Delta T = 10^{-3}$ K applied across a 10-nm-thick AF results in a voltage $\sim\mu$V, which is in the range of that measured by [7]. (See third section of the Supplemental Material [17].) In addition to MnF_2, other materials, such NiO [20] and Cr_2O_3 [1,21], are also possible candidates for the insulating antiferromagnetic layer.

Conclusion and discussion.—In this Letter, we have theoretically demonstrated two methods to realize spin transport in thin antiferromagnetic insulators that do not require the presence of a magnetic field or a ferromagnet. Working from a stochastic Landau-Lifshitz-Gilbert phenomenology, we obtained two key results. First, the spin conductance diverges as the magnetic field approaches the spin-flop transition. Second, the spin Seebeck effect may survive at zero field if the symmetry between antiferromagnetic sublattices is broken at the interface with normal metal contacts. Additionally, we estimated the inverse spin Hall voltages that would be produced by spin and temperature biasing in experiments.

The thin-film approximation, Eqs. (7) to (14), in which the structural transport coefficients consist of contributions from well-defined spin-wave modes, are valid for

thicknesses $d \ll \lambda$. The parameter $\lambda = \sqrt{A/\alpha T}$, which describes the decay of magnons across the thickness of the film, can be estimated from a Heisenberg model on a lattice as $\lambda \sim a\sqrt{T_N/T\alpha}$ (supposing $T \ll H, K$), where T_N is the Néel temperature and a the lattice spacing. For $T \sim T_N/10$, a low damping factor $\alpha \sim 10^{-3}$ and a lattice spacing $a \sim$ nm, for example, λ corresponds to a thickness of ~50 nm, which grows larger at lower temperatures.

The stochastic Landau-Lifshitz-Gilbert phenomenology we employed, Eqs. (2)–(5), may of course be extended to thicker films, resulting in, for example, an exponential decay over the length scale $\lambda^2|k_T| \sim \sqrt{A\chi}/\alpha$ (with $|k_T|$ as the magnon thermal wave vector) rather than an algebraic decay of the spin conductance with distance. Thicker films, however, introduce additional complications, e.g., elastic disorder scattering and phonon-magnon coupling (e.g., phonon drag). Spin-wave interactions (scattering and mean field effects), which are absent in the single-particle treatment above, may change transport at higher spin-wave densities, e.g., at higher temperatures or thicker films or near the spin-flop transition, where the Bose-Einstein divergence may necessitate a many-body treatment, thereby altering the conductance G. The scattering times and length scales over which such effects become important remain an open question. In addition, in our model the transition from the antiferromagnetic to spin-flop phase is second order; the presence of the Dzyaloshinskii-Moriya interaction, spin-wave interactions, or in-plane anisotropy can change critical exponents such as ν in $G \sim (1 - |H|/H_c)^{\nu}$ from its value $\nu = -1$ obtained above or even alter the order of the phase transition, thereby modifying the field dependence of G [22].

This work received funding from the Stichting voor Fundamenteel Onderzoek der Materie (FOM) and the European Research Council via Advanced Grant No. 669442, "Insulatronics."

[1] V. Baltz, A. Manchon, M. Tsoi, T. Moriyama, and T. Ono, arXiv:1606.04284.

[2] R. Gómez-Abal, O. Ney, K. Satitkovitchai, and W. Hübner, Phys. Rev. Lett. **92**, 227402 (2004); T. Kampfrath, A. Sell, G. Klatt, A. Pashkin, S. Mährlein, T. Dekorsy, M. Wolf, M. Fiebig, A. Leitenstorfer, and R. Huber, Nat. Photonics **5**, 31 (2011); T. Satoh, S.-J. Cho, R. Iida, T. Shimura, K. Kuroda, H. Ueda, Y. Ueda, B. A. Ivanov, F. Nori, and M. Fiebig, Phys. Rev. Lett. **105**, 077402 (2010).

[3] P. Wadley *et al.*, Science **351**, 587 (2016); C. Hahn, G. de Loubens, V. V. Naletov, J. Ben Youssef, O. Klein, and M. Viret, Europhys. Lett. **108**, 57005 (2014); H. Wang, C. Du, P. C. Hammel, and F. Yang, Phys. Rev. Lett. **113**, 097202 (2014); T. Moriyama, S. Takei, M. Nagata, Y. Yoshimura, N. Matsuzaki, T. Terashima, Y. Tserkovnyak, and T. Ono, Appl. Phys. Lett. **106**, 162406 (2015); P. Ross, M. Schreier, J. Lotze, H. Huebl, R. Gross, and S. T. B. Goennenwein, J. Appl. Phys. **118**, 233907 (2015); R. Khymyn, I. Lisenkov, V. S. Tiberkevich, A. N. Slavin, and B. A. Ivanov, Phys. Rev. B **93**, 224421 (2016).

[4] P. Yan, X. S. Wang, and X. R. Wang, Phys. Rev. Lett. **107**, 177207 (2011); G. Tatara, Phys. Rev. B **92**, 064405 (2015).

[5] S. T. B. Goennenwein, R. Schlitz, M. Pernpeintner, K. Ganzhorn, M. Althammer, R. Gross, and H. Huebl, Appl. Phys. Lett. **107**, 172405 (2015); L. J. Cornelissen, J. Liu, R. A. Duine, J. B. Youssef, and B. J. van Wees, Nat. Phys. **11**, 1022 (2015); J. Li, Y. Xu, M. Aldosary, C. Tang, Z. Lin, S. Zhang, R. Lake, and J. Shi, Nat. Comm. **7**, 10858 (2016).

[6] W. Lin, K. Chen, S. Zhang, and C. L. Chien, Phys. Rev. Lett. **116**, 186601 (2016).

[7] S. M. Wu, W. Zhang, A. KC, P. Borisov, J. E. Pearson, J. S. Jiang, D. Lederman, A. Hoffmann, and A. Bhattacharya, Phys. Rev. Lett. **116**, 097204 (2016); S. Seki, T. Ideue, M. Kubota, Y. Kozuka, R. Takagi, M. Nakamura, Y. Kaneko, M. Kawasaki, and Y. Tokura, Phys. Rev. Lett. **115**, 266601 (2015).

[8] Y. Ohnuma, H. Adachi, E. Saitoh, and S. Maekawa, Phys. Rev. B **87**, 014423 (2013).

[9] S. M. Rezende, R. L. Rodríguez-Suárez, and A. Azevedo, Phys. Rev. B **93**, 014425 (2016).

[10] L. J. Cornelissen, K. J. H. Peters, G. E. W. Bauer, R. A. Duine, and B. J. van Wees, Phys. Rev. B **94**, 014412 (2016).

[11] S. S. L. Zhang and S. Zhang, Phys. Rev. B **86**, 214424 (2012).

[12] S. Takei, B. I. Halperin, A. Yacoby, and Y. Tserkovnyak, Phys. Rev. B **90**, 094408 (2014).

[13] A. Qaiumzadeh, H. Skarsvåg, C. Holmqvist, and A. Brataas, Phys. Rev. Lett. **118**, 137201 (2017).

[14] R. Cheng, J. Xiao, Q. Niu, and A. Brataas, Phys. Rev. Lett. **113**, 057601 (2014).

[15] A complete treatment of transport generally requires treating the coupled magnetic, phononic, and electronic degrees of freedom of the heterostructure on equal footing. However, if the metallic leads are good spin sinks (so that any spin accumulation driven by magnetic dynamics is quickly relaxed, and $\boldsymbol{\mu}$ is determined exclusively by spin Hall driving) and assuming a large phononic heat conductance throughout the structure, it is reasonable to neglect the feedback on the lead electrons and phonons from the AF spin-wave degrees of freedom in our simple model.

[16] K. M. D. Hals, Y. Tserkovnyak, and A. Brataas, Phys. Rev. Lett. **106**, 107206 (2011).

[17] See Supplemental Material at http://link.aps.org/supplemental/10.1103/PhysRevLett.119.056804 for derivation of spin wave equations of motion, high temperature transport coefficients, and experimental estimates.

[18] A. Kapelrud and A. Brataas, Phys. Rev. Lett. **111**, 097602 (2013).

[19] S. Hoffman, K. Sato, and Y. Tserkovnyak, Phys. Rev. B **88**, 064408 (2013).

[20] A. Prakash, J. Brangham, F. Yang, and J. P. Heremans, Phys. Rev. B **94**, 014427 (2016).

[21] H. Wang, C. Du, P. C. Hammel, and F. Yang, Phys. Rev. B **91**, 220410(R) (2015).

[22] P. C. Hohenberg and B. I. Halperin, Rev. Mod. Phys. **49**, 435 (1977).